

# Conductive Polymer Composites Cathodes for Rechargeable Aqueous Zn-ion Batteries: A Mini-review

Guanjie He<sup>a,b\*</sup>, Yiyang Liu<sup>b</sup>, Daisy E Gray<sup>a</sup>, James Othon<sup>a</sup>

a. School of Chemistry, University of Lincoln, Brayford Pool, Lincoln, LN6 7TS, UK.

b. Department of Chemical Engineering, University College London (UCL), London WC1E 7JE, UK.

Email: [ghe@lincoln.ac.uk](mailto:ghe@lincoln.ac.uk); [g.he@ucl.ac.uk](mailto:g.he@ucl.ac.uk)

**Abstract:** With the supply of lithium resources beginning to dwindle, rechargeable aqueous zinc-ion batteries (AZIBs) have attracted research interests as alternatives to lithium-ion batteries. Developing high-performance and cost-effective cathodes can promote the commercialisation process of AZIBs. Transition metal-based materials, including different phases of vanadium oxides, manganese oxides and Prussian blue analogues are promising candidates due to their reasonable crystal structures to host Zn-ions. However, they are suffering from the low electrical conductivity and structural instability. The modification of these materials by conductive polymers and the formation of composites is demonstrated as promising strategies to solve the problem and improve the cathode performance in AZIBs. In this mini review, we summarize representative advancements of conductive polymer composites as cathodes in AZIBs and provide an insight into their future research directions.

**Keywords:** conductive polymer, Zn-ion battery, cathode, composite

## 1. Introduction

The consumption of fossil fuels deteriorates the environmental pollution, which calls for the significant evolution of renewable energy technologies. The UK has taken the initiative and announced the new Ten Point Plan for a green industrial revolution. The aim is to produce enough offshore wind, quadruple the current production to 40 GW by 2030 [1]. However, renewable energies, such as wind, are not continuously supplied, which means renewable energy production processes are highly erratic. This promotes the requirement for different scales of energy storage devices.

Energy storage technologies continue to evolve and adapt to ever-increasing demands. Lithium-ion batteries (LIBs) occupy a large proportion of the energy storage market and their market shares are still growing exponentially [2]. However, expensive raw materials and the flammable electrolyte inhibits the further development and grid scale storage application of LIBs. The promising alternatives for LIBs are rechargeable aqueous Zn-ion batteries (AZIBs) [3]. Generally, AZIB uses a weak acid aqueous electrolyte, whose charge and energy storage involves the highly reversible stripping/plating of the Zn on the anode and Zn<sup>2+</sup>(de)intercalation on the cathode. Theoretically, zinc is a relatively cheap and low toxic metal, and zinc anodes offer an ultrahigh volumetric capacity of 5855 mAh/cm<sup>3</sup>, compared to that of Li anodes (2061 mAh/cm<sup>3</sup>), due to two-electron transfer per metal ion and relatively higher density. Additionally, the redox potential of Zn/Zn<sup>2+</sup> (-0.76 V vs. standard hydrogen electrode) is suitable for AZIBs to be used in aqueous electrolytes [4]. However, the application of AZIBs is hindered by immature cathode materials due to sluggish kinetics from the strong electrostatic interaction between divalent species and cathode hosts. Generally, there are several suitable crystal structures as cathodes to accommodate Zn ions, which can be mainly classified into vanadium-based ( $\delta$ -Ni<sub>0.25</sub>V<sub>2</sub>O<sub>5</sub>·nH<sub>2</sub>O, NH<sub>4</sub>V<sub>4</sub>O<sub>10</sub>), manganese-based ( $\alpha$ -MnO<sub>2</sub>,  $\gamma$ -MnO<sub>2</sub>,  $\delta$ -MnO<sub>2</sub>), Prussian blue analogue-based (copper hexacyanoferrate, iron hexacyanoferrate) and other transition metal-based (NiCoP, NiCo<sub>2</sub>S<sub>4</sub>, ZnCo<sub>2</sub>O<sub>4-x</sub>) materials [5–9]. But the structural instability, irreversible phase transformation and poor electrical conductivity of typical cathode materials cause routine specific capacity, unsatisfactory rate capability and cycling stability [10]. Recently, we have comprehensively discussed several strategies to improve the performance of AZIBs, including cathode modification through forming composites, electrolyte optimization and device-level innovation [11,12].

Conductive polymers with highly p-conjugated polymeric chains can improve the overall electrical conductivity of composites and provide extra redox couples for semi-conductive electrode materials [13–15]. Representative conductive polymers include polypyrrole, polyacetylene, polyaniline, polythiophene and poly(3,4-ethylenedioxythiophene) polystyrene sulfonate [16,17]. These materials are widely used in supercapacitors and rechargeable batteries due to merits such as easy fabrication, controllable structures, flexibility and high electrical conductivity [18–22]. Recent advancements show the enhanced performance of conductive polymer composites used as AZIB cathode materials; however, their study is immature [23–25].

In this mini-review, we firstly provide synthetic strategies and the structural information of indicative conductive polymers for electrochemical energy storage applications. Then, the progress of the composites composed of conductive polymers with other cathode materials (vanadium-based, manganese-based, Prussian blue analogue-based materials) for AZIBs is discussed. The perspective of this research area is finally provided. This review aims at attracting research interests to boost the further development of low-cost and highly-performed conductive polymer composites in AZIB cathode applications.

## 2. Representative conductive polymers

Conductive polymers can be prepared *via* the controllable oxidation process from chemical and electrochemical processes. By controlling reagents and synthetic conditions, chemical and physical properties, such as nanostructures, chemical stability and electrical conductivity, can be tuned. In this section, normally used conductive polymers will be discussed, previous comprehensive reviews and recent typical examples will be referred.

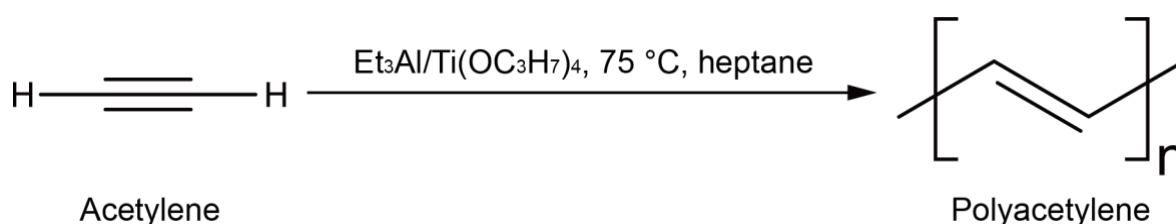


**Figure 1.** Schematic illustration for the typical synthesis of polyacetylene.

### Polyacetylene (PAC)

PAC was firstly proved to transfer from insulating to conductive polymers when certain oxidation or reduction are adopted. The modification of PAC can induce multifunctional behaviours, including enhanced electrical conductivity, by tuning its decorating groups [26]. Polyacetylene derivative polymers are demonstrated to improve the chemistry of the perovskite precursor and boost the performance of solar cells. Enhanced electrical properties can be realized by the synthesis of polyacetylene-like graphene oxide aerogels [27]. Catalytic polymerization, non-catalytic polymerization and precursor-assisted methods are generally used for the synthesis of PAC and its derivatives. One typical synthetic process was developed by Natta (Figure 1), a combination of  $\text{Et}_3\text{Al}$  and  $\text{Ti}(\text{OC}_3\text{H}_7)_4$  with a catalyst molar ratio (Al/Ti) of 2.5 at 75 °C can be used to generate a high yield (98.5% monomer conversion) [28]. More detailed synthetic strategies of PAC are summarized in a recent review [17]. Xu *et al.* developed

the novel synthesis of both cis- and trans-PAC chains on the Cu (110) surface, they provided a new understanding of the structural and electrical properties of trans-PAC in real space. The modification, such as doping, will influence physical or chemical properties of Pac [29]. Shi *et al.* have investigated the effects of iodine doping on the lattice thermal conductivity of oxidized polyacetylene nanofibers [13]. Zhang *et al.* have summarized the nanostructures and doping effects of conductive polymers, including the PAC in their comprehensive review. Due to the relatively low electrical conductivity but good mechanical flexibility, PAC can be used as the carbon source to fabricate suitable carbon materials [14]. Akagi *et al.* developed a morphology-retaining carbonization process to fabricate helical graphite films from iodine-doped helical PAC films [26].

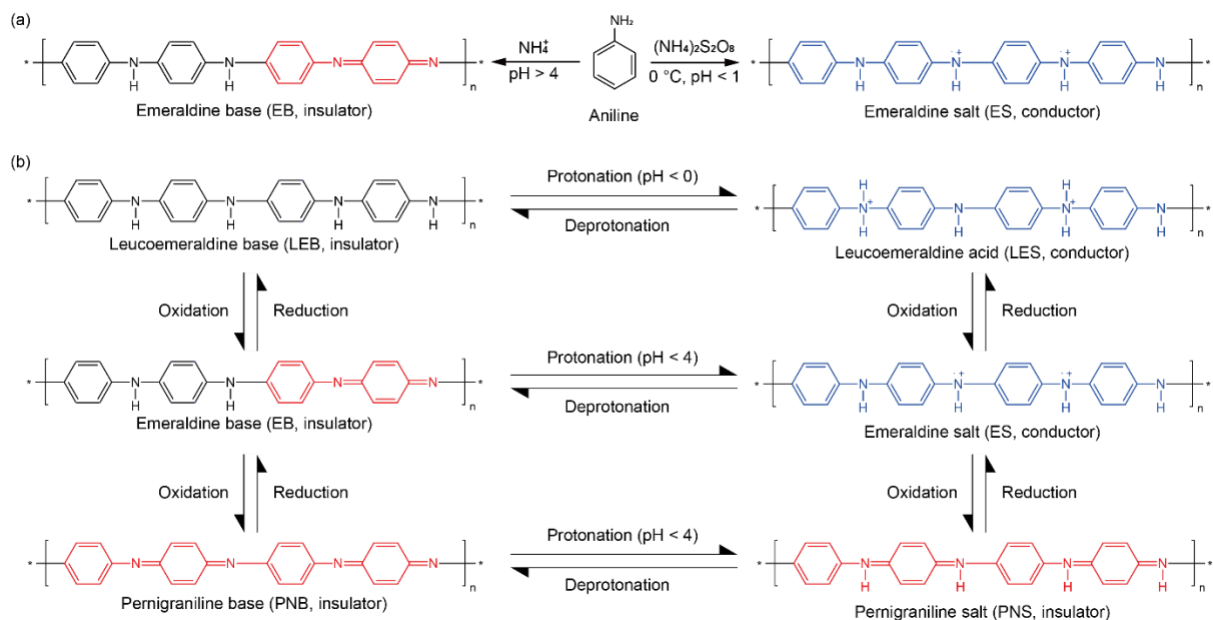


**Figure 2.** Typical synthetic schemes and different types of polyaniline.

## Polyaniline (PANi)

PANi can exist in several forms, which can be classified as Leucoemeraldine (sufficiently reduced state), Emeraldine (mixed reduced and oxidized state), and Pernigraniline (fully oxidized state), according to their different oxidation states (Figure 2). PANi is an insulator when it is fully oxidized in a high pH value. The electrical conductivity of PANi can be tuned by the solvent, when the environmental pH is less than 1, it becomes a conductor or semi-conductor showing higher electrical conductivity. Chemical oxidation strategies are intensively investigated to prepare PANi. In general, aniline monomers and an oxidant (*i.e.* ammonium

persulfate, potassium bichromate, *etc.*) are mixed in an acid solution. The widely used oxidants and suggested reaction conditions are summarized in a recent review by Rout *et al.* Different dimensions of the PANi can be controlled *via* changing synthetic methods, such as electrospinning for manufacturing 1D PANi materials and 3D structures by the template-assisted methods [17,30]. The electrochemical polymerization is suitable for the synthesis of PANi, Xiong *et al.* used anodic electrochemical polymerization to fabricate flexible conductive paper@PANi-vitrimer hybrid electrodes [18]. PANi is proved to exhibit high electrical conductivity *via* the HCl modification. But the conductive PANi is relatively unstable, thus limiting its application scenarios in AZIBs based on mildly acidic electrolytes [31].

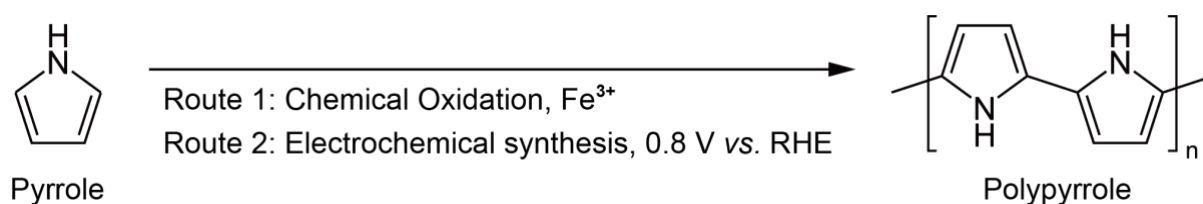


**Figure 3.** The typical synthetic routes for polypyrrole.

### Polypyrrole (PPy)

PPy, composed of conjugated structures with alternative C-C and C=C bonds, is prepared *via* the oxidative polymerization of pyrrole monomers [32]. PPy has one of the highest electrical conductivity compared to other conductive polymers, up to tens or hundreds of S cm<sup>-1</sup> [33]. Chemical synthesis and electrochemical methods are widely used for its preparation (Figure 3). Chemical oxidants, such as the FeCl<sub>3</sub>, are used. The yield and morphology of PPy can be tuned through the ratio of oxidants and monomers, and the reaction condition [34]. Zhi *et al.* have comprehensively summarized the synthetic methods from 1D to 3D dimensions [19]. Recently, Zhai *et al.* have developed an innovative structure, *i.e.* longan-like PPy, through the self-templated strategies [20]. FeCl<sub>2</sub>·4H<sub>2</sub>O and H<sub>2</sub>O<sub>2</sub> were used as the oxidants, and distilled water was used as the reaction media. The longan-like PPy nanosphere can be used as the conductive support to form the core-shell structure with other active materials, thus facilitating the electrochemical performance. By simply changing the reaction time and mixing procedure of reactants, Ji *et al.* obtained the PPy nanospheres [23]. Vapour-phase polymerization is one typical chemical synthesis method for fabricating PPy coating layers on other active materials to improve overall stability and electrical conductivity of electrodes [35]. Tectorum-like PPy thin-layers on α-Fe<sub>2</sub>O<sub>3</sub> nanoarrays were synthesized by using 0.1 mol L<sup>-1</sup> FeCl<sub>3</sub> ethanol solution as the oxidant. Electrochemical oxidation is another widely used process for forming

PPy, which has advantages include high yield, direct film fabrication, and easy-to-control property [22]. The synthetic mechanisms have been intensively investigated and summarized in previous studies and reviews. The electrolyte, substrates and working modes have huge influences on the final products. By controlling counter-anions in the electrochemical oxidation polymerization process, the lateral PPy growth was suppressed and the underlying metal layers during deposition were passivated, which enabled the structures with scalable overall volumes and tunable geometries [36].

### 3. Conductive Polymer Composites

Conductive polymer composites exhibit multiple advantages, including rich active sites and synergistic effects from each component. The energy storage performance of typical cathode materials can be improved *via* the formation of composites. Even though at an early stage, the recent progress of cathode materials for AZIBs formed by conductive polymers and typical cathode candidate composites will be introduced in this section [37].

#### Conductive Polymer Composites with Manganese-based Materials

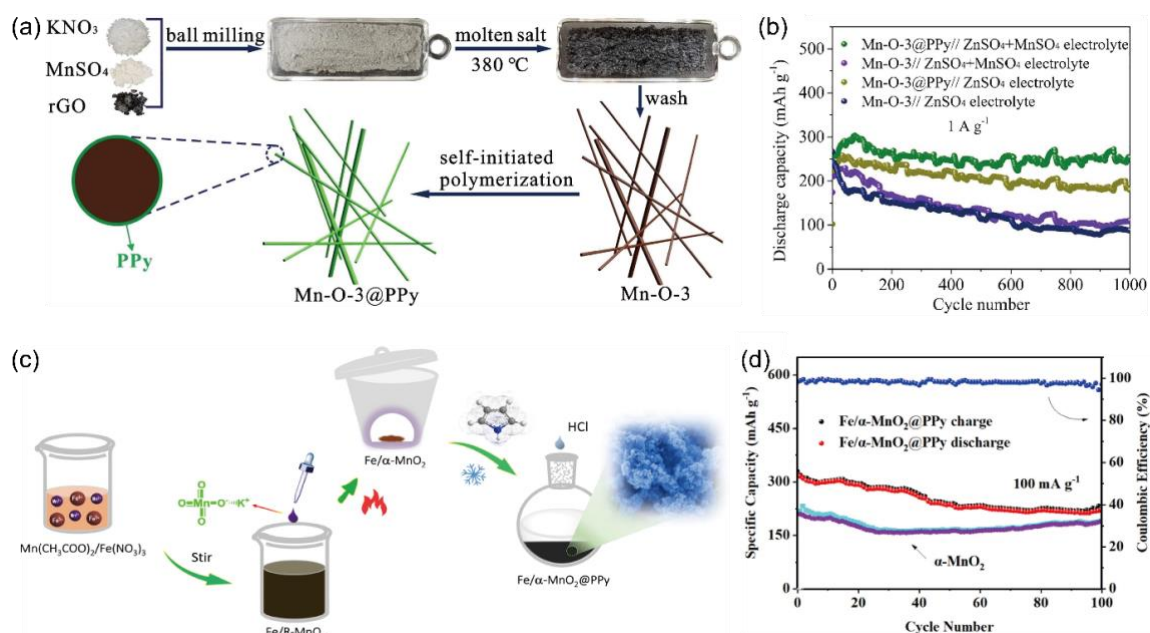


**Figure 4.** Composites with manganese-based cathodes.

(a). Schematic diagram of the Mn-O-3@PPy nanocomposite synthesis; (b). long-term cycling performance of Mn-O-3 and Mn-O-3@PPy at the current density of  $1 \text{ A g}^{-1}$  using two different

electrolytes; Reproduced with permission from [38]. Copyright 2021. Elsevier. (c). The schematic illustration of Fe/ $\alpha$ -MnO<sub>2</sub>@PPy composite preparation; (d) long-term cycling performance of Fe/ $\alpha$ -MnO<sub>2</sub>@PPy and  $\alpha$ -MnO<sub>2</sub> at the current density of 100 mA g<sup>-1</sup>. Reproduced with permission from [39]. Copyright 2021. Elsevier.

Manganese-based materials are widely used due to their low cost and environmental friendly features. In addition, the variety in the valence states of Mn (II, III, IV, VII) and diversity in crystal structures, nano/micro morphology and porosity further broaden the application profile of manganese-based materials. However, the use of manganese-based materials at the cathode of AZIBs has been hampered by the poor electrical conductivity, which results in slow reaction kinetics, especially on commercial high-loading electrodes [40]. The structural instability arises from the manganese oxide dissolution and deposition during the cycling performance test at the electrode-electrolyte interface [41]. Although some strategies have been proposed, such as the use of electrolytes with Mn<sup>2+</sup> additives, the underlying mechanisms have not been thoroughly investigated [11]. In fact, it is still difficult to fully prove whether the mechanism of Mn additives is the extra capacity contribution caused by manganese deposition or simply inhibiting the dissolution of manganese.

The improved electrical conductivity and reduced dissolution phenomena were reported for MnO<sub>2</sub>/Mn<sub>2</sub>O<sub>3</sub> nanocomposites coated with PPy (Figure 4a, b) [38]. The material was prepared using a scalable molten salt synthesis followed by the self-initiated polymerization. The composites exhibited a much higher electrical conductivity than pure MnO<sub>2</sub> (24.1 S cm<sup>-1</sup> and 10<sup>-5</sup>~10<sup>-6</sup> S cm<sup>-1</sup>, respectively), which was reflected by its superior rate capability. The alleviated dissolution of the composite was revealed by its 107.4% capacity retention after 1000 cycles at 3 A g<sup>-1</sup> (compared to only 33.3% retention for Mn-O-3), and after 500 cycles at the current density of 1 A g<sup>-1</sup> (compared to 10.01% for Mn-O-3), in a 5.42% atomic ratio of manganese to zinc in the electrolyte. The further investigation can be conducted to understand the activation period and detailed reaction mechanisms of this composite material.

Besides improving electrical conductivity and stability, composites of manganese-based materials with conductive polymers have been proved to exhibit an increased number of active sites for pseudocapacitive charge storage. This effect has been reported in a PPy-coated/MnO<sub>2</sub> nanowire within carbon nanotube composites (CNT/MnO<sub>2</sub>-PPy) [42]. By transforming the equation relating the peak current to the scan rate ( $i=av^b$ ) in the form of  $\log(i) = b \log(v) + \log(a)$ , cyclic voltammetry data was used to evaluate the electrochemical kinetics of



CNT/MnO<sub>2</sub> and optimized CNT/MnO<sub>2</sub>-PPy cathodes. A plot of  $\log(i)$  against  $\log(v)$  gives a slope with a gradient equivalent to  $b$ . When  $b = 1$ , the measured current is controlled by the capacitive behaviour of the material, and when  $b = 0.5$ , it is controlled by the diffusion of ions. For the CNT/MnO<sub>2</sub> materials, the cathodic peaks relating to H<sup>+</sup> and Zn<sup>2+</sup> insertion have corresponding  $b$  values of 0.54 and 0.34 respectively, therefore the process is dominated by a diffusion-controlled process. The increase in  $b$  values for the same peaks for CNT/MnO<sub>2</sub>-PPy to 0.74 and 0.41 respectively suggests a larger contribution from surface-controlled pseudocapacitive behaviour, and therefore indicates additional active sites for the surface ion absorption and desorption, can be induced on the MnO<sub>2</sub>-PPy interface.

The morphology of conductive polymer composites containing manganese-based materials can be tuned based on the synthetic conditions, which also influences the final performance. A MnO<sub>x</sub>/PPy composite was synthesized using a simple, efficient, and scalable one-step inorganic/organic interface reaction (Figure 4c) [39]. In addition to the reduced dissolution of MnO<sub>x</sub> into the electrolyte, the stability and improved capacity of the composite was credited to its porous structure, which can alleviate the possible volume change that occurs during cycling (Figure 4d). The stability is demonstrated by the specific capacity retention of 107% after 1000 cycles at 6 A g<sup>-1</sup> compared to the 35<sup>th</sup> cycle [41]. Compared to both  $\alpha$ -MnO<sub>2</sub> and Fe-doped  $\alpha$ -MnO<sub>2</sub>, Fe/ $\alpha$ -MnO<sub>2</sub>@PPy was found to have a larger surface area, and its mesoporous structure was expected to allow better electrolyte infiltration and provide additional active sites for the adsorption and desorption of Zn<sup>2+</sup> and H<sup>+</sup>. The composite achieved a higher specific capacity of 200 mAh g<sup>-1</sup> at 100 mA g<sup>-1</sup> compared to  $\alpha$ -MnO<sub>2</sub>, which achieved the specific capacity of 175 mAh g<sup>-1</sup> [39].

### **Conductive Polymer Composites with Vanadium-based Materials**

Two methods that have been found to improve the performance of materials with 1D tunnel-type vanadium oxides are: (1) increasing the tunnel size, which leads to faster diffusion kinetics, and (2) stabilizing the tunnel structure, which leads to better cycling stability [6]. Increasing the rate of Zn<sup>2+</sup> diffusion prevents the severe lattice change of cathodes, which ultimately avoids irreversible phase changes [43]. Conductive polymers PANi, and Poly(3,4-ethylenedioxythiophene) (PEDOT) have been intercalated into vanadium-based materials, thus expanding the tunnel size and preventing the collapse of structures [44,45].



The interplanar distance within the crystal lattice of ammonium vanadate (NVO) was increased from 7.8 Å to 10.8 Å by the simultaneous polymerization of EDOT and the insertion of PEDOT into NVO *via* a redox reaction (Figure 5a) [46]. PEDOT-NVO hybrid materials achieved a higher capacity of 356.8 mAh g<sup>-1</sup> at the current density of 0.05 A g<sup>-1</sup> than that of pure NVO (264.2 mAh g<sup>-1</sup>), and retained 94.1% specific capacity after 5,000 cycles at 10 A g<sup>-1</sup>, demonstrating its excellent stability. The experimental results showed the enlargement of the interplanar distance resulted in easier transport of Zn<sup>2+</sup> ions through the structure. DFT calculations showed a lower kinetic energy barrier for the insertion of Zn<sup>2+</sup> ions for the PEDOT-NVO materials as a result of the generating oxygen vacancies.

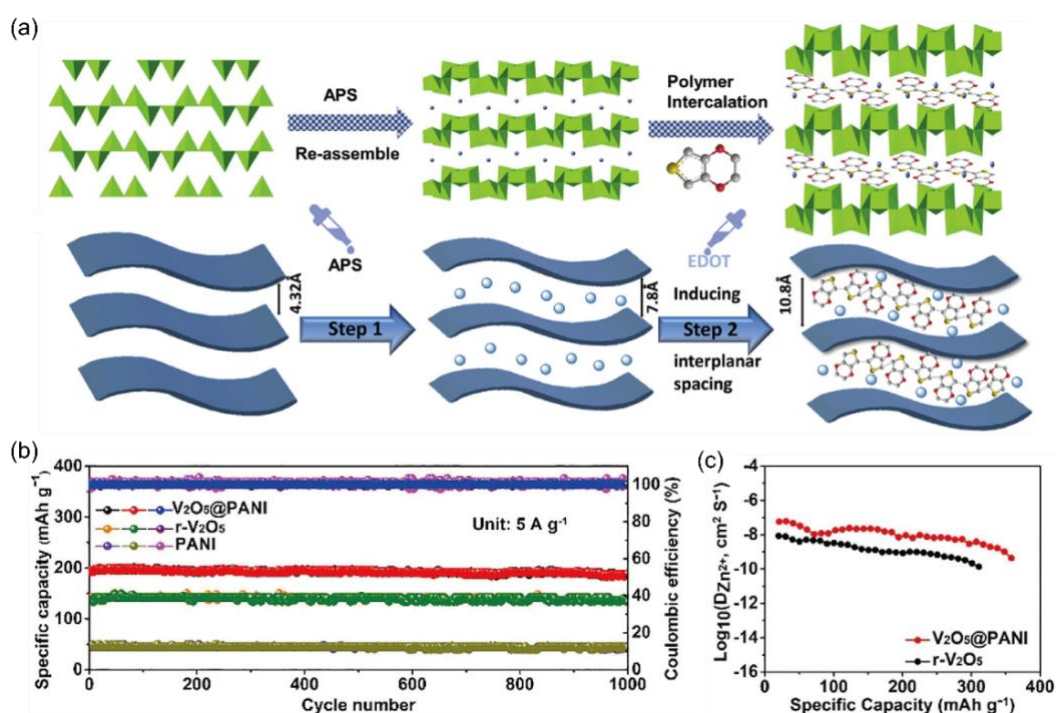


**Figure 5.** Composites with vanadium-based cathodes.

(a). Schematic diagram of the preparation and structural changes of the PEDOT-Intercalation NVO-layered material . Reproduced with permission from [46]. Copyright 2020. Elsevier.

(b). Long-term cycling stability of V<sub>2</sub>O<sub>5</sub>@PANI, r-V<sub>2</sub>O<sub>5</sub>, and PANi at 5 A g<sup>-1</sup>; (c). diffusivity of Zn<sup>2+</sup> in V<sub>2</sub>O<sub>5</sub>@PANI and r-V<sub>2</sub>O<sub>5</sub>. Reproduced with permission from [47]. Copyright 2020. American Chemical Society.

The favourable synergistic effects that can occur in conductive polymer composites were observed in a V<sub>2</sub>O<sub>5</sub>@PANI nanocomposite. The porous material was prepared using a simple organic and inorganic hybridization method, and its electrochemical performance was compared to r-V<sub>2</sub>O<sub>5</sub> and PANI electrodes (Figure 5b, c) [47]. The V<sub>2</sub>O<sub>5</sub>@PANI nanocomposite

achieved a higher specific capacity of  $361 \text{ mAh g}^{-1}$  at  $0.1 \text{ A g}^{-1}$  than r- $\text{V}_2\text{O}_5$  and PANI alone, indicating that the combination of the two materials in a composite results in better properties. Its stability was demonstrated by the retention of 93.8% of its capacity over 1000 cycles. Faster diffusion kinetics were observed with the calculated diffusion coefficient of  $\text{Zn}^{2+}$  for  $\text{V}_2\text{O}_5@\text{PANi}$  (between  $1.18 \times 10^{-7}$  and  $9.1 \times 10^{-10} \text{ S cm}^{-1}$ ) larger than that of r- $\text{V}_2\text{O}_5$ .

Creating vanadium materials with mixed valence states, specifically including  $\text{V}^{4+}$ , demonstrated better electrochemical performances. This improved performance was reported for PEDOT-vanadium oxide (VO) [48]. Once EDOT monomers had been intercalated into the VO material, they were polymerized using a hydrothermal method. Upon the oxidation of EDOT monomers,  $\text{V}_2\text{O}_5$  was partially reduced, resulting in mixed valence states of  $\text{V}^{5+}/\text{V}^{4+}$ . Alongside the electrically conductive nature of the PEDOT, the creation of the mixed valence states are proved to have improved electrical conductivity of the composite materials compared to  $\text{V}_2\text{O}_5$ , and therefore improved the reaction kinetics. The electrical conductivities of PEDOT-VO and  $\text{V}_2\text{O}_5$  are reported as  $1.17 \times 10^{-4} \text{ S cm}^{-1}$  and  $6.79 \times 10^{-6} \text{ S cm}^{-1}$ , respectively. The fast kinetics related to the PEDOT-VO composite is evidenced by its high rate capability of  $175 \text{ mAh g}^{-1}$  at the current density of  $50 \text{ A g}^{-1}$ .

### Conductive Polymer Composites with Prussian Blue Analogues

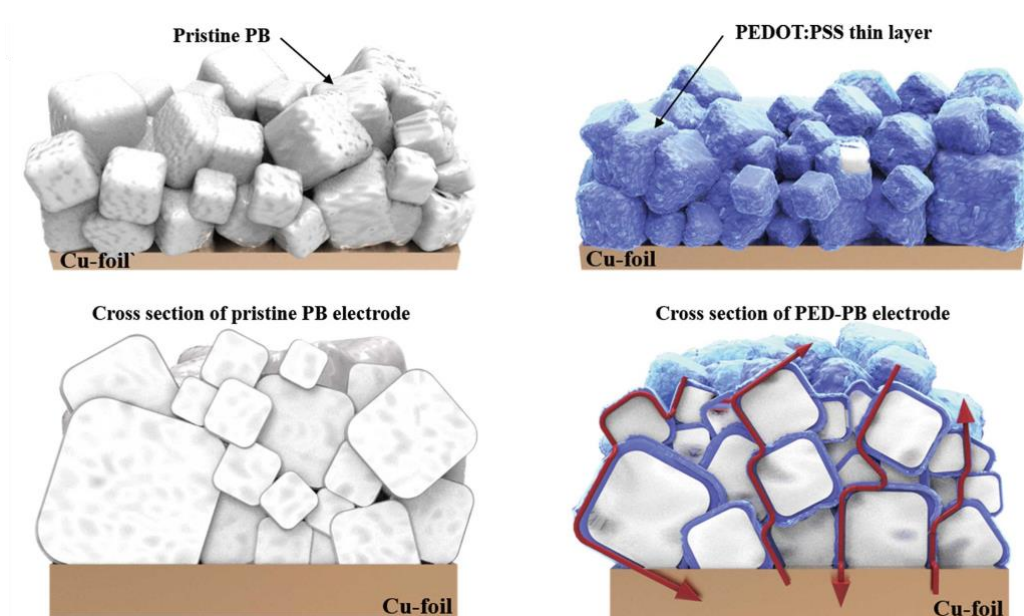


**Figure 6.** Schematic diagram of PED-PB synthesized *via* one-pot coating process. Reproduced with permission from [49]. Copyright 2019. Elsevier.

Prussian blue analogue (PBA) is the simplest metal-organic framework, whose nominal formula is  $A_xM_1[M_2(CN)_6]_z \cdot wH_2O$ , where A represents an alkali metal and M represents transition metal elements. PBAs are promising cathode candidates for electrochemical energy storage devices, due to their remarkable power density, open frameworks, extremely low cost, and simple synthetic routes. Currently, PBA-based cathodes are extensively studied in both aqueous systems, organic electrolyte systems and solid-state electrolyte systems [50,51]. Based on reported findings regarding the investigation of conductive polymer composites with PBA-based cathode materials in other types of secondary batteries, it can be suggested that the performance of PBAs may be improved through the formation of composites with conductive polymers for ZIB applications. Similar to manganese and vanadium-based materials, PBAs suffer from poor electrical conductivity. Furthermore, the presence of  $[M(CN)_6]^{3-}$  vacancies often found to occur in PBAs result in positively charged defects which reduce specific capacity, and associated coordinated water molecules can hinder ion transportation, leading to the poor performance such as low Coulombic efficiency.<sup>11</sup> To the best of our knowledge, there is almost no report about using conductive polymers and PBAs composite cathodes in AZIBs, and only one monomer of conductive polymer intercalated cathode was reported. Very recently, phenylamine (PA)-intercalated  $VOPO_4 \cdot 2H_2O$  showed varied interlayer space of the structures, and the intercalation of PA molecules also significantly increases the hydrophobicity, resulting in inhibiting the decomposition or dissolution of  $VOPO_4 \cdot 2H_2O$  and dramatically improving stability over 2000 cycles at the current density of  $5.0 \text{ A g}^{-1}$  with a capacity retention of  $\sim 200 \text{ mAh g}^{-1}$  [49]. The experimental and theoretical results demonstrate the interlayer space of  $16.5 \text{ \AA}$  can improve the  $Zn^{2+}$  diffusion and result in the ultrahigh diffusion coefficient of  $\sim 5.7 \times 10^{-8} \text{ cm s}^{-1}$ . Monitoring PA within structures can be carried out to check if any polymerization happening during the battery operation. Another example is the use of modified conductive polymers for dual-ion AZIBs. Jiang *et al.* tailored the linking patterns of polypyrene and electronic structures as  $Cl^-$ -hosting cathodes for dual-ion AZIBs [50]. The 1,3,6,8-linking pattern formed the cross-linked polypyrenes showing an extended conjugation degree, a porous structure and high HOMO level and the expanded HOMO orbital distribution. The optimized polypyrene shows a high specific capacity of  $180 \text{ mAh g}^{-1}$  at the current density of  $50 \text{ mA g}^{-1}$  and highly stable cyclabilities of 800 cycles at  $50 \text{ mA g}^{-1}$  and 38,000 cycles at  $3000 \text{ mA g}^{-1}$ .

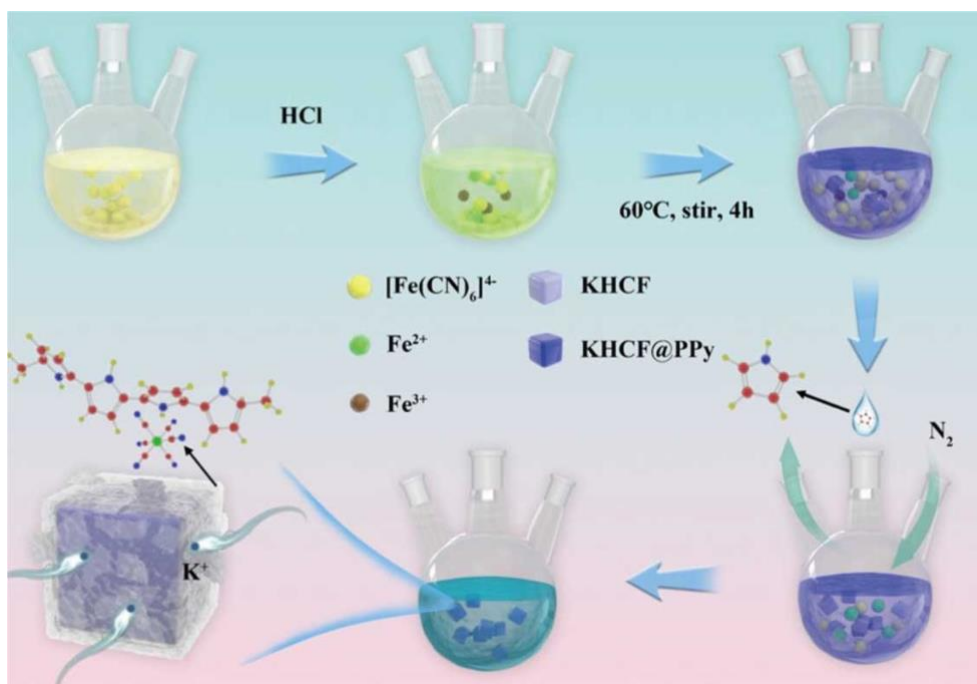


**Figure 7.** Schematic diagram of PPy-modified potassium-rich iron hexacyanoferrate (KHCF@PPy). Reproduced with permission from [52]. Copyright 2019. American Chemical Society.

The composites of PBAs and conductive polymers are used for other batteries. It was reported that in the application of PBAs as cathode materials for sodium ion batteries, capacity and rate capability were improved by creating a PEDOT:PSS (PSS = poly(4-styrenesulfonate)) shell over PB nanocubes. A one-pot synthetic process was used to produce the PED-PB material with a uniform shell of polymer, the thickness of which was easily controlled by altering concentration (Figure 6) [51]. Compared to pristine PB nanocubes, the PED-PB (3.0 wt%) material achieved a higher reversible capacity (123.41 mAh  $\text{g}^{-1}$  and 130.94 mAh  $\text{g}^{-1}$  respectively, both at 12.2 mA  $\text{g}^{-1}$ ), and better rate capability (80.1% and 86.0% reversible capacity maintained respectively, both at 1220 mA  $\text{g}^{-1}$ ). The enhanced performance of PED:PB was attributed to the improvement in electrical conductivity observed when using a conductive polymer to create a composite material. The inclusion of PPy can not only increase electrical conductivity, it also reduced the amount of vacancies and related coordinated water content of PBA materials for the application in potassium ion batteries. A potassium-rich iron hexacyanoferrate composite (KHCF@PPy) was compared to pure KHCF (Figure 7), and it was calculated that it had fewer  $[\text{Fe}(\text{CN})_6]^{4-}$  vacancies (0.03 vs. 0.14 vacancies per molecule of material), and a corresponding lower coordinated water content (0.84  $\text{H}_2\text{O}$  molecules per

molecule of materials vs. 1.68 H<sub>2</sub>O molecules per molecule of materials) [52]. This difference in the vacancy number was due to the difference in the degree of oxidative polymerization of PPy, suggesting that vacancies in PBAs can be controlled through synthetic methods and the use of polymers. The reduced number of vacancies and coordinated water content correlated to higher Coulombic efficiency of 72.67% compared to 64% for pure KHCF. Therefore, similar materials design strategies can be adopted to the future work of cathode design for AZIBs. **The adaptability of different conductive polymers and PBAs can be studied systematically as cathodes in AZIBs.**

#### **4. Conclusion and outlook**

Although there are intensive studies of the synthesis of conductive polymer composites and their application in energy storage and conversion fields, the specific use of conductive polymer composites as cathode materials for AZIBs is at an early stage. The critical understanding of conductive polymers in suitable AZIB electrolytes should be conducted in the future research, including the discovery of stable electrolyte components and suitable potential window, possible electrochemical reactions, and cycling stability.

Both *in-situ* and multi-step formation of composites consisting of conductive polymers and conventional cathode materials are reported, however, synthetic strategies are underdeveloped to obtain specific structures of cathode materials for AZIBs, such as different dimensions and self-standing electrodes of conductive polymer composites, thus further improving the charge transfer process and stability for continuous Zn<sup>2+</sup> storage. Suitable conductive polymers and typical AZIB cathode materials are needed to be discovered and chemical interactions between conductive polymers and AZIB cathode materials, especially under working conditions, should be investigated.

The comprehensive charge storage mechanism needs to be investigated. Conductive polymers are demonstrated to be excellent candidates for pseudocapacitive materials, such as surface redox reactions with H<sup>+</sup> or other cations from the electrolyte. Their synergistic effects with typical AZIB cathode materials need to be studied. Therefore, *operando* and *ex-situ* materials characterisations need to be performed in the future work, including X-ray diffraction, X-ray photoelectron spectroscopy and X-ray absorption spectroscopy to understand the phase and chemical environment transformation, and electron microscopes for structural evolution and stability.



Multiscale simulation work will facilitate the understanding of mechanisms in the future work. Density functional theory can be used to understand electronic structures, formation energy, stable voltage range, theoretical capacity, ion transport kinetics, and phase transition during  $\text{Zn}^{2+}$  ion (de)intercalation processes of conductive polymer composite cathodes. Molecular dynamics can simulate the evolution of system particles, visualise the path of ion migration in long time scales, and calculate the diffusion coefficient along with the stability of materials. It can help to understand the collaborative diffusion mechanism of ions (e.g.  $\text{Zn}^{2+}$  and  $\text{H}^+$ ), which are crucial for mechanistic understanding of charge storage processes and deepening the current understanding for AZIBs.

In summary, future work can focus on combining both experimental and theoretical efforts to promote the development of conductive polymer composites for AZIBs

### **Declaration of competing interest**

The authors declared no competing interests.

### **Acknowledgements**

The authors acknowledged the Engineering and Physical Sciences Research Council (EP/V027433/1; EP/T518177/1) and the Royal Society (RGS\R1\211080) for funding support.

### **References**

- [1] HM Government, The Ten Point Plan for a Green Industrial Revolution, (2020), pp. 1–38.
- [2] X. Guo, Z. Zhang, J. Li, N. Luo, G.-L. Chai, T. S. Miller, F. Lai, P. Shearing, D. J.L. Brett, D. Han, Z. Weng, G. He, I.P. Parkin, Alleviation of Dendrite Formation on Zinc Anodes via Electrolyte Additives, *ACS Energy Lett.*, 6 (2021), pp. 395–403.
- [3] H. Dong, J. Li, S. Zhao, F. Zhao, S. Xiong, D. J.L. Brett, G. He, I. P. Parkin, An anti-aging polymer electrolyte for flexible rechargeable zinc-ion batteries, *J. Mater. Chem. A*, 8 (2020), pp. 22637–22644.

- [4] Y. Jiao, L. Kang, J. Berry-Gair, K. McColl, J. Li, H. Dong, H. Jiang, R. Wang, F. Corà, D. J.L. Brett, G. He, I. P. Parkin, Enabling stable MnO<sub>2</sub> matrix for aqueous zinc-ion battery cathodes, *J. Mater. Chem. A*, 8 (2020), pp. 22075–22082.
- [5] J. Li, K. McColl, X. Lu, S. Sathasivam, H. Dong, L. Kang, Z. Li, S. Zhao, A. G. Kafizas, R. Wang, D. J.L. Brett, P.R. Shearing, F. Corà, G. He, C. J. Carmalt, I. P. Parkin, Multi-Scale Investigations of  $\delta$ -Ni<sub>0.25</sub>V<sub>2</sub>O<sub>5</sub>·nH<sub>2</sub>O Cathode Materials in Aqueous Zinc-Ion Batteries, *Adv. Energy Mater.*, 10 (2020), pp. 1–14.
- [6] J. Ding, H. Gao, D. Ji, K. Zhao, S. Wang, F. Cheng, Vanadium-based cathodes for aqueous zinc-ion batteries: From crystal structures, diffusion channels to storage mechanisms, *J. Mater. Chem. A*, 9 (2021), pp. 5258–5275.
- [7] Y. Zhao, Y. Zhu, X. Zhang, Challenges and perspectives for manganese-based oxides for advanced aqueous zinc-ion batteries, *InfoMat.*, 2 (2020), pp. 237–260.
- [8] Q. Li, X. Rui, D. Chen, Y. Feng, N. Xiao, L. Gan, Q. Zhang, Y. Yu, S. Huang, A High-Capacity Ammonium Vanadate Cathode for Zinc-Ion Battery, *Nano-Micro Lett.*, 12 (2020), p. 3.
- [9] L. Wang, J. Zheng, Recent advances in cathode materials of rechargeable aqueous zinc-ion batteries, *Mater. Today Adv.*, 7 (2020), p. 100078.
- [10] N. Borchers, S. Clark, B. Horstmann, K. Jayasayee, M. Juel, P. Stevens, Innovative zinc-based batteries, *J. Power Sources*, 484 (2021), p. 229309.
- [11] Y. Liu, G. He, H. Jiang, I. P. Parkin, P. R. Shearing, D. J.L. Brett, Cathode Design for Aqueous Rechargeable Multivalent Ion Batteries: Challenges and Opportunities, *Adv. Funct. Mater.*, 31 (2021), p. 2010445.
- [12] H. Dong, J. Li, J. Guo, F. Lai, F. Zhao, Y. Jiao, D.J.L. Brett, T. Liu, G. He, I.P. Parkin, Insights on Flexible Zinc-Ion Batteries from Lab Research to Commercialization, *Adv. Mater.*, 20 (2021), p. 2007548.
- [13] Y. Shi, G. Yu, Designing Hierarchically Nanostructured Conductive Polymer Gels for Electrochemical Energy Storage and Conversion, *Chem. Mater.*, 28 (2016), pp. 2466–2477.



- [14] J. Xie, P. Gu, Q. Zhang, Nanostructured Conjugated Polymers: Toward High-Performance Organic Electrodes for Rechargeable Batteries, *ACS Energy Lett.*, 2 (2017), pp. 1985–1996.
- [15] H.E. Katz, P.C. Searson, T.O. Poehler, Batteries and charge storage devices based on electronically conducting polymers, *J. Mater. Res.*, 25 (2010), pp. 1561–1574.
- [16] Y. Shi, L. Peng, Y. Ding, Y. Zhao, G. Yu, Nanostructured conductive polymers for advanced energy storage, *Chem. Soc. Rev.*, 44 (2015), pp. 6684–6696.
- [17] K. Namsheer, C.S. Rout, Conducting polymers: a comprehensive review on recent advances in synthesis, properties and applications, *RSC Adv.*, 11 (2021), pp. 5659–5697.
- [18] C. Xiong, M. Li, W. Zhao, C. Duan, L. Dai, M. Shen, Y. Xu, Y. Ni, A smart paper@polyaniline nanofibers incorporated vitrimer bifunctional device with reshaping, shape-memory and self-healing properties applied in high-performance supercapacitors and sensors, *Chem. Eng. J.*, 396 (2020), p. 125318.
- [19] Y. Huang, H. Li, Z. Wang, M. Zhu, Z. Pei, Q. Xue, Y. Huang, C. Zhi, Nanostructured Polypyrrole as a flexible electrode material of supercapacitor, *Nano Energy*, 22 (2016), pp. 422–438.
- [20] W. He, G. Zhao, P. Sun, P. Hou, L. Zhu, T. Wang, L. Li, X. Xu, T. Zhai, Construction of Longan-like hybrid structures by anchoring nickel hydroxide on yolk-shell polypyrrole for asymmetric supercapacitors, *Nano Energy*, 56 (2019), pp. 207–215.
- [21] S. Chen, H. Cheng, D. Tian, Q. Li, M. Zhong, J. Chen, C. Hu, H. Ji, Controllable Synthesis, Core-Shell Nanostructures, and Supercapacitor Performance of Highly Uniform Polypyrrole/Polyaniline Nanospheres, *ACS Appl. Energy Mater.*, 4 (2021), pp. 3701–3711.
- [22] L. Wang, H. Yang, X. Liu, R. Zeng, M. Li, Y. Huang, X. Hu, Constructing Hierarchical Tectorum-like  $\alpha$ -Fe<sub>2</sub>O<sub>3</sub>/PPy Nanoarrays on Carbon Cloth for Solid-State Asymmetric Supercapacitors, *Angew. Chemie - Int. Ed.*, 56 (2017), pp. 1105–1110.
- [23] C. Zhang, W. Ma, C. Han, L.W. Luo, A. Daniyar, S. Xiang, X. Wu, X. Ji, J.X. Jiang, Tailoring the linking patterns of polypyrrole cathodes for high-performance aqueous Zn dual-ion batteries, *Energy Environ. Sci.*, 14 (2021), pp. 462–472.

- [24] F. Wan, L. Zhang, X. Wang, S. Bi, Z. Niu, J. Chen, An Aqueous Rechargeable Zinc-Organic Battery with Hybrid Mechanism, *Adv. Funct. Mater.*, 28 (2018), p. 1804975.
- [25] F. Guo, S. Gao, C. Ji, H. Mi, H. Li, W. Zhang, H. Pang, Finely crafted polyaniline cathode for high-performance flexible quasi-solid-state Zn-ion battery, *Solid State Ionics*, 364 (2021), p. 115612.
- [26] K. Bi, A. Weathers, S. Matsushita, M.T. Pettes, M. Goh, K. Akagi, L. Shi, Iodine doping effects on the lattice thermal conductivity of oxidized polyacetylene nanofibers, *J. Appl. Phys.*, 114 (2013), p. 194302.
- [27] T. Masuda, Substituted Polyacetylenes: Synthesis, Properties, and Functions, *Polym. Rev.*, 57 (2017), pp. 1–14.
- [28] H. Shirakawa, E.J. Louis, A.G. MacDiarmid, C.K. Chiang, A.J. Heeger, Synthesis of electrically conducting organic polymers: Halogen derivatives of polyacetylene, (CH)<sub>x</sub>, *J. Chem. Soc. Chem. Commun.*, (1977), pp. 578–580.
- [29] S. Wang, Q. Sun, O. Gröning, R. Widmer, C.A. Pignedoli, L. Cai, X. Yu, B. Yuan, C. Li, H. Ju, J. Zhu, P. Ruffieux, R. Fasel, W. Xu, On-surface synthesis and characterization of individual polyacetylene chains, *Nat. Chem.*, 11 (2019), pp. 924–930.
- [30] X. X. Wang, G. F. Yu, J. Zhang, M. Yu, S. Ramakrishna, Y. Z. Long, Conductive polymer ultrafine fibers via electrospinning: Preparation, physical properties and applications, *Prog. Mater. Sci.*, 115 (2021), p. 100704.
- [31] D. Zhang, On the conductivity measurement of polyaniline pellets, *Polym. Test*, 26 (2007), pp. 9–13.
- [32] O. N. Efimov, R. Chem, Related content Polypyrrole: a conducting polymer; its synthesis, properties and applications Polypyrrole : a conducting polymer; its synthesis, properties and applications, (1997).
- [33] R. Ansari, Polypyrrole Conducting Electroactive Polymers: Synthesis and Stability Studies, *E-Journal Chem.*, 3 (2006), pp. 186–201.
- [34] S. Rapi, V. Bocchi, G. P. Gardini, Conducting polypyrrole by chemical synthesis in water, *Synth. Met.*, 24 (1988), pp. 217-221.

- [35] S. Sadki, P. Schottland, N. Brodie, G. Sabouraud, The mechanisms of pyrrole electropolymerization, *Chem. Soc. Rev.*, 29 (2000), pp. 283–293.
- [36] M. Synodis, J.B. Pyo, M. Kim, X. Wang, M.G. Allen, Lithographically patterned polypyrrole multilayer microstructures via sidewall-controlled electropolymerization, *J. Micromechanics Microengineering*, 31 (2021), 025008.
- [37] P. Ruan, X. Xu, X. Gao, J. Feng, L. Yu, Y. Cai, X. Gao, W. Shi, F. Wu, W. Liu, X. Zang, F. Ma, X. Cao, Achieving long-cycle-life Zn-ion batteries through interfacial engineering of MnO<sub>2</sub>-polyaniline hybrid networks, *Sustain. Mater. Technol.*, 28 (2021), e00254.
- [38] A. Huang, W. Zhou, A. Wang, M. Chen, J. Chen, Q. Tian, J. Xu, Self-initiated coating of polypyrrole on MnO<sub>2</sub>/Mn<sub>2</sub>O<sub>3</sub> nanocomposite for high-performance aqueous zinc-ion batteries, *Appl. Surf. Sci.*, 545 (2021), p. 149041.
- [39] J. W. Xu, Q. L. Gao, Y. M. Xia, X. S. Lin, W. L. Liu, M. M. Ren, F. G. Kong, S. J. Wang, C. Lin, High-performance reversible aqueous zinc-ion battery based on iron-doped alpha-manganese dioxide coated by polypyrrole, *J. Colloid Interface Sci.*, 598 (2021), pp. 419–429.
- [40] D. T. Tung, H. M. Nguyet, N. T. Dung, H. T. Dung, N. T. Yen, N. B. Thanh, P. N. Hong, P. Van Hoi, N. Van Quynh, P. N. Minh, L.T. Lu, Pulse Electrodeposition of Polyaniline/Mn-Fe Binary Metal Hydroxide Composite Cathode Material for a Zn-Ion Hybrid Supercapacitor, *J. Electron. Mater.*, 50 (2021), pp. 4407-4414.
- [41] Z. Li, Y. Huang, J. Zhang, S. Jin, S. Zhang, H. Zhou, One-step synthesis of MnO:X/PPy nanocomposite as a high-performance cathode for a rechargeable zinc-ion battery and insight into its energy storage mechanism, *Nanoscale*, 12 (2020), pp. 4150–4158.
- [42] Y. Zhang, G. Xu, X. Liu, X. Wei, J. Cao, L. Yang, Scalable In Situ Reactive Assembly of Polypyrrole-Coated MnO<sub>2</sub> Nanowire and Carbon Nanotube Composite as Freestanding Cathodes for High Performance Aqueous Zn-Ion Batteries, *ChemElectroChem*, 7 (2020), pp. 2762–2770.
- [43] B. Tang, L. Shan, S. Liang, J. Zhou, Issues and opportunities facing aqueous zinc-ion batteries, *Energy Environ. Sci.*, 12 (2019), pp. 3288–3304.

- [44] W. Li, C. Han, Q. Gu, S. L. Chou, J. Z. Wang, H. K. Liu, S.X. Dou, Electron Delocalization and Dissolution-Restraint in Vanadium Oxide Superlattices to Boost Electrochemical Performance of Aqueous Zinc-Ion Batteries, *Adv. Energy Mater.*, 10 (2020), pp. 1–9.
- [45] J. Kim, S. H. Lee, C. Park, H. S. Kim, J.H. Park, K. Y. Chung, H. Ahn, Controlling Vanadate Nanofiber Interlayer via Intercalation with Conducting Polymers: Cathode Material Design for Rechargeable Aqueous Zinc Ion Batteries, *Adv. Funct. Mater.*, 26 (2021), pp. 1–15.
- [46] D. Bin, W. Huo, Y. Yuan, J. Huang, Y. Liu, Y. Zhang, F. Dong, Y. Wang, Y. Xia, Organic-Inorganic-Induced Polymer Intercalation into Layered Composites for Aqueous Zinc-Ion Battery, *Chem.*, 6 (2020), pp. 968–984.
- [47] Y. Du, X. Wang, J. Man, J. Sun, A novel organic-inorganic hybrid  $V_2O_5$ @polyaniline as high-performance cathode for aqueous zinc-ion batteries, *Mater. Lett.*, 272 (2020), p. 127813.
- [48] S. Li, X. Wei, C. Wu, B. Zhang, S. Wu, Z. Lin, Constructing Three-Dimensional Structured  $V_2O_5$ /Conductive Polymer Composite with Fast Ion/Electron Transfer Kinetics for Aqueous Zinc-Ion Battery, *ACS Appl. Energy Mater.*, 4 (2021), pp. 4208–4216.
- [49] D.S. Kim, H. Yoo, M.S. Park, H. Kim, Boosting the sodium storage capability of Prussian blue nanocubes by overlaying PEDOT:PSS layer, *J. Alloys Compd.*, 791 (2019), pp. 385–390.
- [50] L. Ma, S. Chen, N. Li, Z. Liu, Z. Tang, J.A. Zapien, S. Chen, J. Fan, C. Zhi, Hydrogen-Free and Dendrite-Free All-Solid-State Zn-Ion Batteries, *Adv. Mater.*, 32 (2020), p. 1908121.
- [51] L. Ma, S. Chen, X. Li, A. Chen, B. Dong, C. Zhi, Liquid-Free All-Solid-State Zinc Batteries and Encapsulation-Free Flexible Batteries Enabled by In Situ Constructed Polymer Electrolyte, *Angew. Chemie Int. Ed.*, 59 (2020), pp. 23836–23844.
- [52] Q. Xue, L. Li, Y. Huang, R. Huang, F. Wu, R. Chen, Polypyrrole-Modified Prussian Blue Cathode Material for Potassium Ion Batteries via in Situ Polymerization Coating, *ACS Appl. Mater. Interfaces.*, 11 (2019), pp. 22339–22345.

